Robust Ferroelectricity with Suppressed Leakage Current in Ultrathin HfO_2/ZrO_2 nanolaminates

Guan Feng, Xiaodong Wang, Yize Sun, Yingfen Wei, Hao Jiang*
Frontier Institute of Chip and System, Fudan University, Shanghai, China 200438
Email: haoj@fudan.edu.cn

HfO_2-based ferroelectric devices have attracted significant research interests for next-generation memory and computing due to their high CMOS compatibility and low power consumption [1-3]. In most of the previous studies, the HfO_2-based ferroelectric films have a typical thickness of 10 nm and coercive field (Ec) of ~ 1.5 MV/cm. Further scaling down the thickness allows lower operating voltage and hence their integration onto advanced technology nodes. Here, we systematically studied ultrathin ferroelectric HfO_2/ZrO_2 nanolaminate (NL) films. The capacitors based on 4 nm NL film demonstrated high ferroelectricity (double remnant polarization ($2P_r$) ~ 20 μC/cm^2), low coercive voltage (V_c ~ 0.5 V), and >50 X decrease in leakage current when compared with the conventional $Hf_{0.5}Zr_{0.5}O_2$ solid solution (SS) film.

Fig. 1 (a) and (b) schematically illustrate the structure of fabricated capacitors with SS and NL films respectively. The detailed process flow is shown in Fig. 1(c). 40 nm TiN was sputtered onto the SiO_2/Si substrates as the bottom electrode. The HZO SS film was prepared with a 1:1 HfO_2:ZrO_2 ALD cycle ratio, while the HfO_2/ZrO_2 NL film has a periodicity of HfO_2(0.5nm)-ZrO_2(0.5nm). 40nm TiN top electrodes were patterned by photolithography and lift-off. Finally, a post metallization annealing (PMA) was performed at 500/600 ^{0}C for 30s in N_2 ambient by RTP. During electrical measurements, the top electrodes were biased with the bottom ones grounded.

Fig. 2(a) shows the typical DC leakage curves from the capacitors based on 10 nm SS film, 6 nm SS and NL film with their corresponding polarization-voltage (P-V) curves exhibited in Fig. 2(b). The leakage of the 6 nm NL film is 3-4 times lower than that of the 6 nm SS film and 10 times lower than the widely used 10 nm SS film. In addition, the 6 nm NL film shows similar $2P_r$ and E_c as the 10 nm SS one, leading to a clear reduction in the operating voltage.

To further explore the benefit of our ferroelectric HfO_2/ZrO_2 NL film, capacitors with 4 nm SS and NL films were fabricated and electrically characterized. Both kinds of capacitors show typical anti-ferroelectric behaviors at the pristine state. The 4 nm NL film shows no difference in leakage before and after wake-up while ~10 and >50 times decrease when compared with the 4 nm SS film at the pristine and woken-up state respectively (Fig. 3(a)). A deformed P-E behavior was obtained from the SS film due to its high leakage (Fig. 3(b)) while our NL film shows a typical ferroelectric hysteresis with $2P_r$ ~ 20 μC/cm^2 and low V_c of ~ 0.5V (Fig. 3(c)).

The speed, endurance, and retention properties of our ultrathin ferroelectric NL films will also be presented. In addition, we will present our studies on their conduction mechanism which can elaborate the origin of the improvement in leakage.

[1] T. M, et al. IEDM Tech. Dig., Oct. 2020, pp. 18.4.1–18.4.5 (2020). [2] M. H. Park, et al. MRS Commun., vol. 8, no. 3, pp. 795–808, (2018). [3] M. H. Park, et al. Adv.

Mater. 27, 1811 (2015)

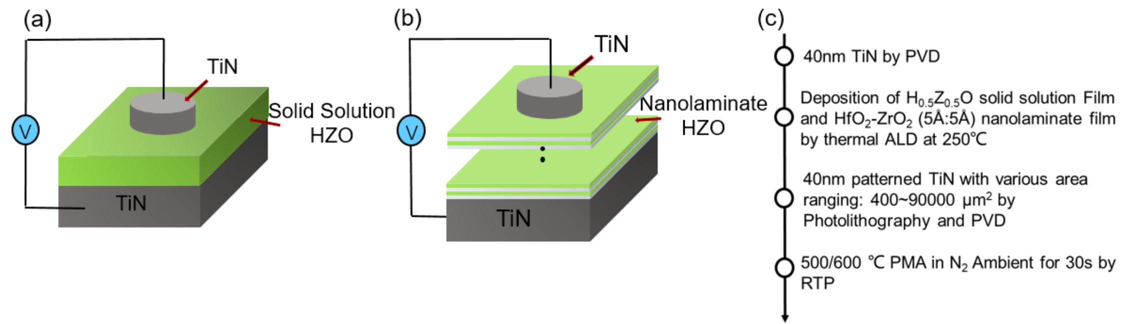

Figure 1. Schematic view of devices with (a) conventional $Hf_{0.5}Zr_{0.5}O_2$ solid solution (SS) film and (b) novel HfO_2/ZrO_2 nanolaminate (NL) films. (c) Fabrication process flow of ferroelectric capacitors using TiN electrodes.

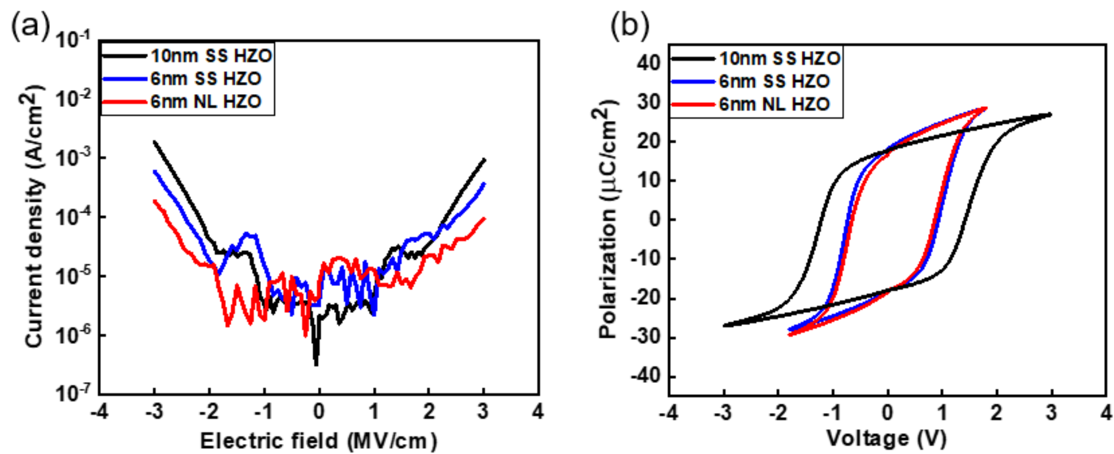

Figure 2. (a) Typical DC leakage and (b) P-V curves from ferroelectric capacitors based on 10 nm SS film, 6 nm SS and NL films.

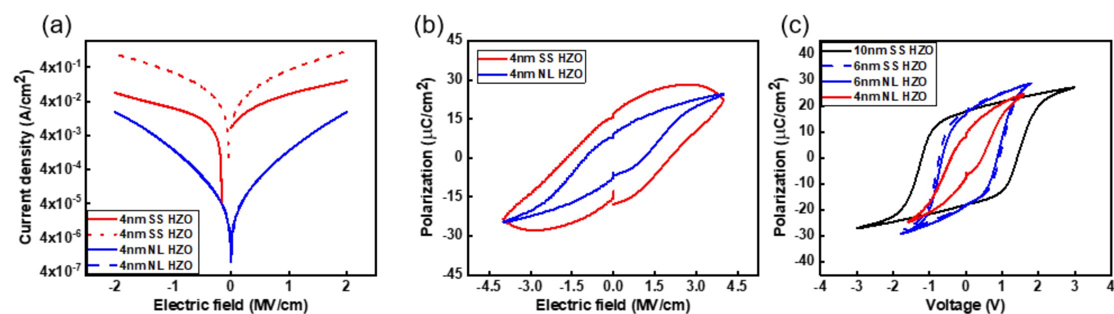

Figure 3. (a) Typical DC leakage curves from ferroelectric capacitors based on 4 nm SS and NL films (Solid line: pristine state; dash line: after wake-up). (b) Typical P-E curves from ferroelectric capacitors based on 4 nm SS and NL films after wake-up. (c) The comparison of P-V loops from ferroelectric capacitors based on SS and NL films with varied thicknesses.